# LINEAR OPTICS MEASUREMENTS IN THE ESRF BOOSTER

Y. Papaphilippou, L. Farvacque, E. Plouviez, ESRF, Grenoble, France
A. Mostacci, A. Patriarca, Università La Sapienza, Roma, Italy

## *Abstract*

A series of experiments was conducted in the ESRF booster in order to measure its linear optics. A steerer response matrix was developed and used to optimise the orbit correction at injection by producing a refined model. This matrix was also used to measure the beta functions along the accelerating cycle and the steerer calibration. Dispersion was measured with classical RF scans and compared to the model. Finally, chromaticity measurements were performed for different sextupole settings enabling their calibration and optimisation.

## INTRODUCTION

The ESRF Booster [1], a 300 m fast sychnotron, accelerates electrons, coming from a 200 MeV linac, to a final energy of 6 GeV in 50 ms and extracts them into the ESRF storage ring with a repetition rate of 1-10 Hz. The lattice is based on a FODO structure with a missing dipole, forming 39 cells respecting a 3-fold symmetry. Twelve 2 m-long dispersion free straight sections are used for accommodating two 352.2 MHz RF cavities, the injection and the extraction elements. Each magnet family is powered by a 10 Hz resonant "white circuit". Chromaticity is corrected along the cycle by two families of sextupoles whereas the orbit is only corrected at injection with 78 independently powered steerers. A set of basic Booster parameters is displayed in Table 1.

Table 1: ESRF Booster parameters.

| | |
|---|---|
| Circumference $C$ | 299.622 m |
| Extraction Energy $E_{ext}$ | 6 GeV |
| Nominal current $I_{nom}$ | 5 mA - 0.1 mA |
| Harmonic number $h$ | 352 |
| Accelerating cycle $t_{cycle}$ | 50 ms |
| Working point $(Q_x, Q_y)$ | (11.8, 9.8) |
| Momentum compaction factor $\alpha_c$ | $9.6 \ 10^{-3}$ |
| Emittances at 6GeV $(\epsilon_{x;ext}, \epsilon_{y;ext})$ | (120,3) nm rad |
| Energy spread at 6GeV $(\delta E/E)_{ext}$ | $1.1 \ 10^{-3}$ |
| Bunch length $l_s$ | 2.61 cm (87 ps) |

The "cleaning" of parasitic bunches by resonantly exiting the unwanted particles in order to direct them to a scraper, is essential for the good performance of the few bunch modes in the storage ring, where a demanding purity of better than $10^{-7}$ is required for time-domain dependent experiments. The installation of an efficient bunch cleaning system in the booster is necessary for the implementation of continuous injection (with open front-ends), even in these filling modes. During 2004, the necessary hardware was successfully installed and tested [2] and, at present, the procedure is under the optimisation phase. Meanwhile, it became apparent that the knowledge, monitoring and control of several booster optics parameters is essential for the good performance of the cleaning. In this paper, we report on the developments and measurements undertaken for the improvement and characterisation of the booster, namely the orbit correction algorithm, the measurement of the optics functions, the establishment of a correct optics model and the beam based calibration of the sextupoles through chromaticity measurements.

## ORBIT RESPONSE MATRIX

The orbit correction is performed at injection by powering 78 DC dipole correctors distributed symmetrically (apart from a few exceptions), near the focusing and defocusing quadrupoles. The orbit is monitored by 75 Beam Position Monitors (BPM) [3] placed in between the quadrupoles and steerers. The orbit position can be monitored simultaneously in 6 different moments during the acceleration cycle. An orbit correction control application is available whereby different methods [4] can be applied such as closed bumps, harmonic, or most effective steerer. A correction algorithm based on Singular Value Decomposition (SVD) used at the ESRF storage ring was recently ported to the booster. The efficiency of the algorithm is heavily dependent on the determination of a booster optics model including the steerer calibration. It was thus necessary to measure a steerer response matrix, based on which, a machine model can be constructed and the optics determined.

This matrix is constructed by applying a current change to each steerer and measuring the position difference $\Delta x(s)$ on all BPM around the ring. The orbit distortion $\Delta x$ in the BPM at position $s$ is $\Delta x(s) = \Delta\theta(s_0)\frac{\sqrt{\beta(s)\beta(s_0)}\cos(|\mu_{s,s_0}|-\pi Q)}{2\sin(\pi Q)} + \frac{\eta_x(s)\eta_x(s_0)}{(\alpha_c-1/\gamma^2)C}$, where $\Delta\theta(s_0)$ is the dipole kick from a steerer at position $s_0$, $\beta, \eta, \mu$ the beta, dispersion and phase functions, $Q$ the betatron tune and $\alpha_c$ the momentum compaction factor. The last term is a small correction due to the momentum change induced by the kick at dispersive locations. Ignoring this term a complementary beta functions estimation can be obtained by the estimating the beta functions that reproduce all displacements around the ring, through an iterative procedure.

The model is calibrated for a given time in the cycle by fitting the theoretical horizontal and vertical response matrices to the data collected on the Booster. The measured response matrices are averaged over the 3 super-periods to reduce the effect of magnet imperfections. The rms deviation between the elements of both matrices is minimised by ad-
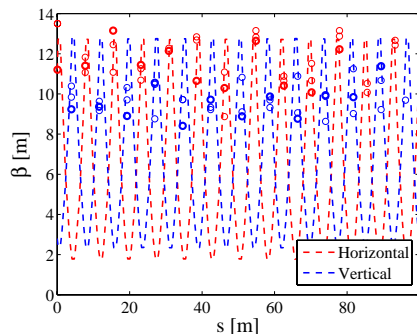
Figure 1: Horizontal (blue) and vertical (red) beta functions as estimated by the fitted model (curves) and measured directly by the values of the orbit shifts (points).

justing 4 parameters : the strengths of the two quadrupole families (QF and QD) and the strengths of the two steerer families (horizontal and vertical). In Fig. 1, we present the beta functions around the ring as estimated by the fitted model (curves) and these measured through the displacements around the ring. The beta variation seems to be less than 10%.

## DISPERSION MEASUREMENTS
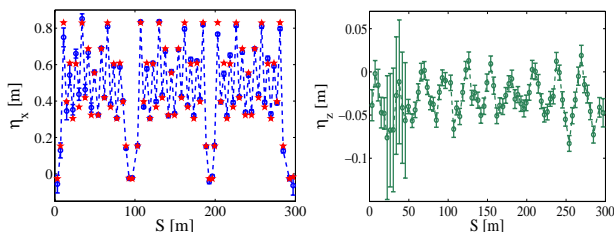


Figure 2: Theoretical (red stars) and measured (blue circles) horizontal [top] and measured vertical [bottom] dispersion around the ring, at 1ms after injection.

Besides the construction of a good optical booster model, the knowledge of dispersion is necessary for an accurate orbit correction algorithm, based on the response matrix analysis. Dispersion around the booster can be estimated by measuring the orbit displacement for different RF frequencies and using the theoretical value of the momentum compaction (Tab. 1) in order to connect the frequency change with the momentum spread. The orbit displacement is $\delta = -\frac{\eta}{\alpha_c} \frac{\delta f_{RF}}{f_{RF}}$. Dispersion is determined by the slope of the linear fit between orbit displacements on both planes, and the momentum spread. The fit works quite well for small momentum spreads of the order of $\pm 2 \times 10^{-3}$

Fig. 2 shows the horizontal (left) and vertical dispersion (right), as measured at 1 ms after injection, in all the BPM around the booster, starting from injection. The error bars correspond to the estimated error of the linear data fit. The red stars in the top plot represent the theoretical value of the horizontal dispersion as estimated by MAD [5] using a super-periodic model. Ideally, vertical dispersion should be zero. For both planes, the error is bigger near the injection area, due to the limited reproducibility of the injection conditions. However, the size of the error bars is small in
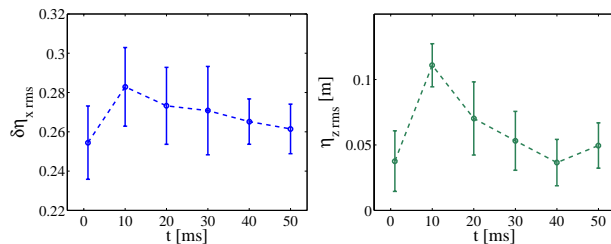


Figure 3: Horizontal [left] and vertical [right] rms dispersion difference between the theoretical and measured values, along the acceleration cycle.

the case of the horizontal dispersion (less than 10% of the values). The theoretical values are quite close to the measured ones, considering the fact that the model does not take into account real orbit displacements which produce additional dispersion. This effect should be responsible for the non-zero vertical dispersion.

In Fig. 3, we present the difference between the measured and theoretical rms values of the dispersion around the ring, as they evolve during the accelerating cycle. The error bars represent one standard deviation of the orbit shift around the ring. For both planes, there is a pick of the rms difference around 10 ms. One can note that at that instant, the tune values are $(Q_x, Q_y) = (11.84, 9.81)$ [6]. On the other hand the vertical chromaticity approaches also its pick value of $-10.8$. The combination of the two effects may move off-momentum particles close to the integer resonance, thus creating transverse orbit distortion and optics functions beating, reflected in the dispersion variation with respect to the theoretical super-periodic model. However, the average fluctuation of the measurements with respect to the theoretical model is quite small.

## SEXTUPOLE CALIBRATION

Two families of sextupoles, 21 horizontal and 30 vertical, make it possible to control chromaticity in the booster. In order to control it automatically, especially during the bunch cleaning procedure, it is necessary to calibrate the sextupole strengths. Recall that the induced chromaticity by a pair of sextupole families with strengths $S_{h,v}(s,t)$ is given by $\xi_{x,z}^{\text{sext}}(t) = \frac{1}{4\pi} \oint [\pm S_h(s,t) \mp S_v(s,t)] \eta_x(s)\beta_{x,z}(s)ds$, where the + or - contribute to horizontal and vertical chromaticity, respectively. Based on the value of the beta functions, each family has a major effect to horizontal or vertical chromaticity. The chromaticity sextupole strengths can be represented as a linear function of the sextupole currents $I_{h,v}^{\text{sext}}(t) = I_{h,v}^{\text{DC}} - I_{h,v}^{\text{AC}} \cos(\omega t + \phi_{x,z})$, $S_{h,v}(t) = \frac{C_s I_{h,v}^{\text{sext}}(t)}{B\rho}$ , where $C_s$ is the unknown calibration factor, which depends on the magnet characteristics. The sextupole calibration factor can be estimated by measuring the induced chromaticity for different sextupole current settings. In the booster, where the current changes along the cycle, the calibration factor can be estimated for different time instants, in order to obtain better statistics.

For small variations of the RF frequency, the chromatic-

ity should be a linear function of the tune shift, $\xi_{x,y} = -\alpha_c f_{RF} \frac{\Delta Q_{x,y}}{\Delta f_{RF}}$. The chromaticity can be measured from the slope between the tune-shift determined by the tune monitor versus the momentum spread. The measurement error is estimated by the error in the slope of the linear data fit. For different values of the sextupole currents (DC and AC part), a chromaticity change of $\delta\xi_{x,z}(t) = \pm C_s \frac{\delta I_{h,v}^{AC,DC}(t)}{4\pi B\rho} \oint \eta_x(s)\beta_{x,z}(s)ds$, will be induced at time $t$ along the accelerating cycle. The integral involving the optics functions is computed using the booster MAD model. As the horizontal (vertical) beta functions are high in the location of "focusing" ("defocusing") sextupole families, it is better to consider changes of the horizontal (vertical) chromaticity for the calibration of the "focusing" (defocusing) sextupole components.
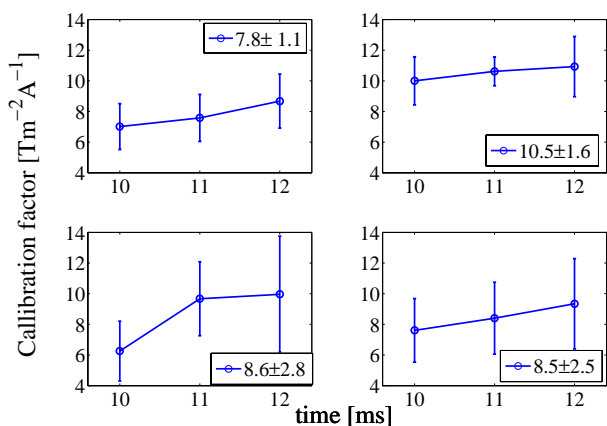


Figure 4: Calibration factor for the DC (left) and the AC (right) component of the focusing (upper) and defocusing (lower) sextupoles from 10 to 12 ms of the cycle.

From previous measurements [6], it is known that the tune (and thus the chromaticity) can be quite unstable, during the very first ms of the cycle, due to injection fluctuations. On the other hand, close to the extraction area, the chromaticity is not sensitive to sextupole current variations limited to some tenths of Amps, for not producing beam losses, at injection. Taking this into account, the time span between 10 and 12ms was chosen for the chromaticity measurements and calibration estimation. This time range is close enough to injection for the chromaticity variation to be significant and long enough after it in order to avoid injection instabilities.

In Fig. 4, we present the final results in the calibration of the DC (left) and AC (right) part of the calibration factor components for both sextupole families, during 3 consecutive moments of the accelerating cycle. The error bars correspond to the error estimated by the linear fit of data. The mean values and standard deviation are also found on these plots. The calibration factors of all components are close to each other and the error on the estimation is less than 20%. The main contribution to the uncertainty when evaluating the calibration factor is attributed to the limited synchronisation of the different equipments and, in particular the timer set-point and the tunes measurements. In fact, it may

occur that the time set-point has not been reached before the measurement is triggered due to network delays. Another problem occurs due to the existence of a phase shift in the AC part of the sextupole current $\phi_{x,z}$, which in our case, was set to be equal to zero. A phase shift may also exist in the dipole magnets, slightly changing the estimation of the magnetic rigidity $B\rho$. These phase shifts may account for the slight dependence of the calibration factor with time (see Fig. 4)

## CONCLUSION AND PERSPECTIVES

The project of parasitic bunches cleaning in the booster triggered a series of linear optics measurements in order to characterise the synchrotron along its accelerating cycle. An orbit application was developed using the SVD approach. For this, a linear optics model was constructed based on a steerer response matrix analysis. A complementary result of this analysis was the estimation of the beta functions along the booster. A further refinement of the optics model can be achieved by considering quadrupole alignment and gradient errors. Dispersion measurements were also performed, in order to refine the orbit correction algorithm. All the measurements showed a quite good agreement of measured dispersion with the theoretical values with a difference of less than 10% around the ring and along the cycle. The existence of vertical dispersion and the increase of its rms values in both planes, at 10 ms has to be studied more in depth. A more accurate model with the real orbit and finer turn-by-turn measurements using the booster strip-line may further explain this behaviour.

Chromaticity measurements were also performed for different values of the DC and AC components of the two families of chromaticity sextupoles in order to perform a beam based calibration. The results were satisfactory considering the limited synchronisation of the equipments. The recent addition of a system for tune determination along the whole cycle in a single injection will decrease the acquisition time considerably and will allow the performance of multiple measurements for a better statistical evaluation of data [7]. A further improvement can be achieved by using orbit measurements for different dipole settings in order to determine the magnetic rigidity phase factor. A similar approach with the chromaticity measurements, will enable the estimation of the phase shift associated with the sextupole current AC component, thus reducing the uncertainty in the determination of the calibration factors.

## REFERENCES

[1] ESRF Foundation Phase Report, Chapter III, ESRF, February 1987; J. M. Filhol, EPAC 1992, Berlin, Germany, p. 471.

[2] E. Plouviez, N. Michel, EPAC 2004, Lucerne, Switzerland, p. 2341.

[3] K. Scheidt, F. Loyer, EPAC 1992, Berlin, Germany, p.1121.

[4] M.G. Minty, F. Zimmermann, Measurement and control of charged particle beams, Springer, 2003.

[5] C. Iselin, H. Grote, CERN/SL/90–13 (AP), Rev.5, 1996.

[6] Y. Papaphilippou, et al., PAC 2003, Portland, USA, p. 851.

[7] J.-M. Koch, et al., DIPAC 2005, in preparation.